

Support information

In situ Grown Lanthanum Sulfide/Molybdenum Sulfide Hybrid Catalyst for Electrochemical Hydrogen Evolution

Xinran Ding,^a Tao Yang,^{a,*} Wenxian Wei,^b Yihui Wang,^a Kai Xu,^a Zizheng Zhu,^a Hong Zhao,^a Tingting Yu^a and Dongen Zhang^a

^a Jiangsu Key Laboratory of Marine Bioresources and Environment, Co-Innovation Center of Jiangsu Marine Bio-industry Technology, Jiangsu Ocean University, Lianyungang 222005 (China)

^b Testing Center, Yangzhou University, Yangzhou 225009 (China)

CORRESPONDING AUTHOR

Correspondence and requests for materials should be addressed to Tao Yang
(yangtao_hit@163.com)

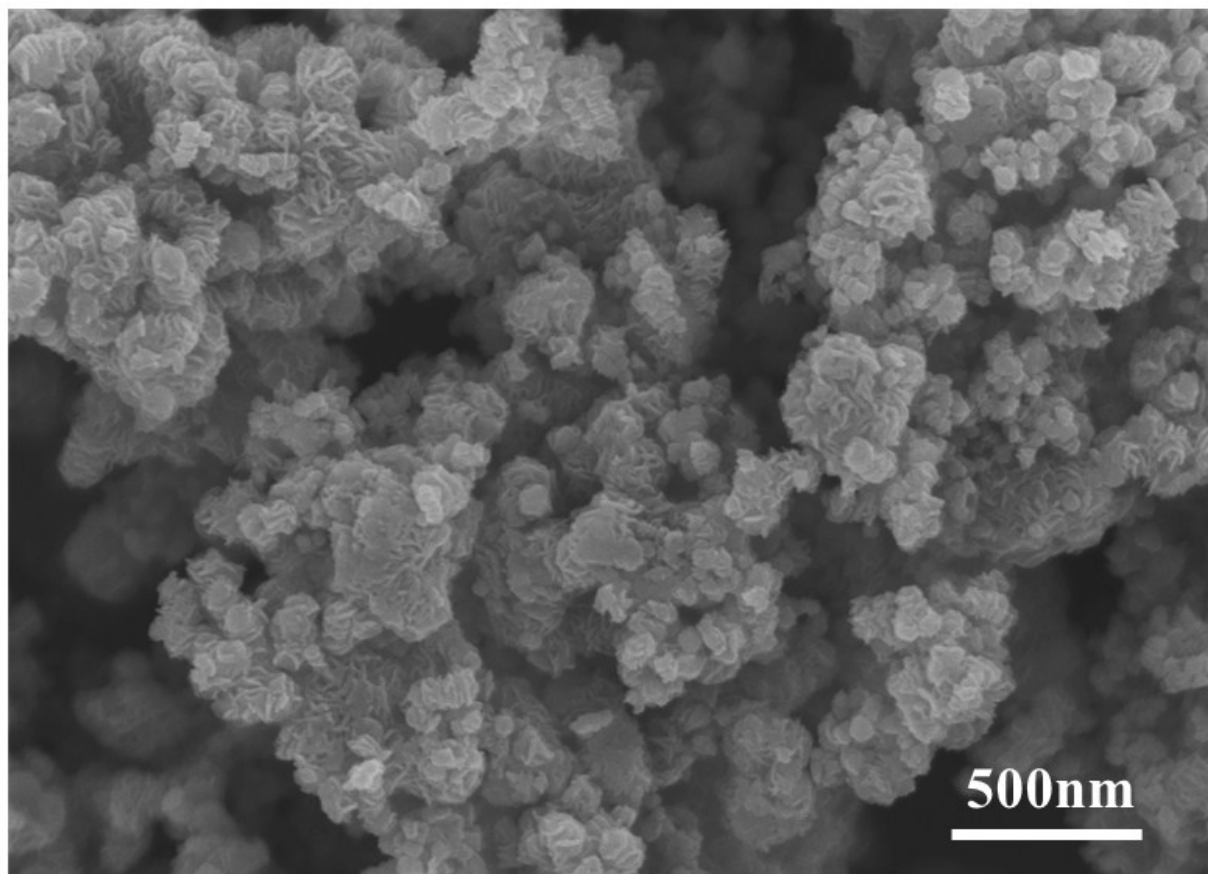


Fig. S1 SEM image of $\text{La}_2\text{S}-\text{MoS}_2$.

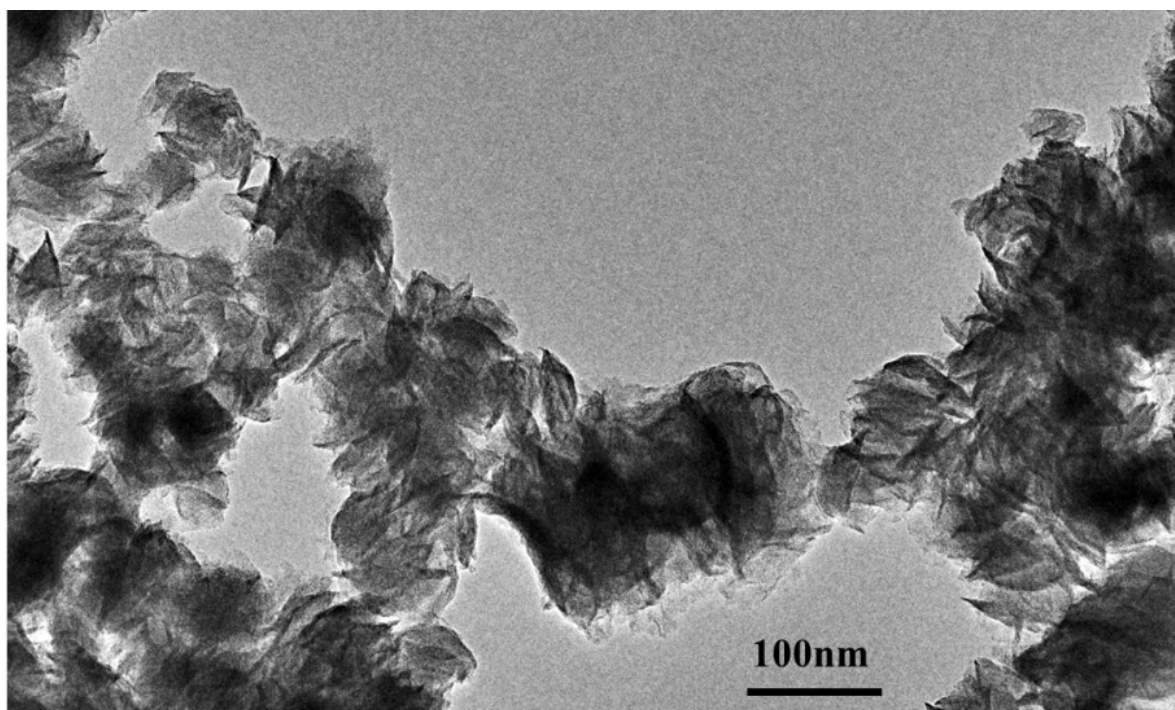


Fig. S2 TEM image of $\text{La}_2\text{S}-\text{MoS}_2$.

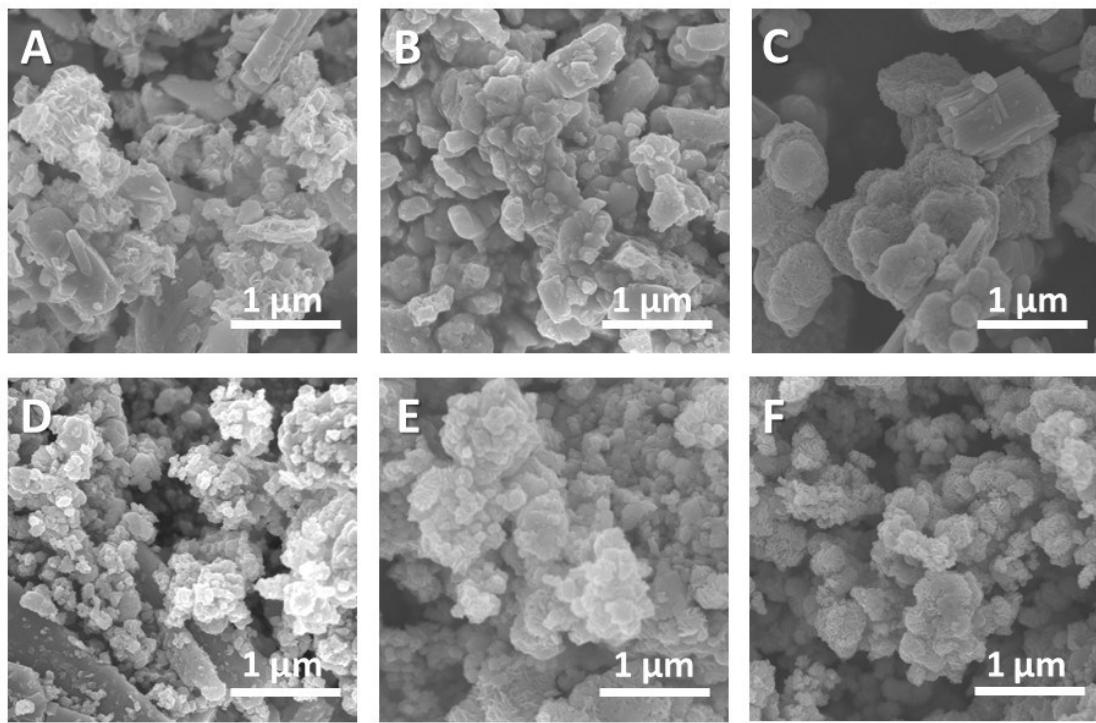


Fig. S3 SEM images of (A) La_2S_3 -MoS₂-1, (B) La_2S_3 -MoS₂-2, (C) La_2S_3 -MoS₂-3, (D) La_2S_3 -MoS₂-4, (E) La_2S_3 -MoS₂-5, (F) La_2S_3 -MoS₂-6.

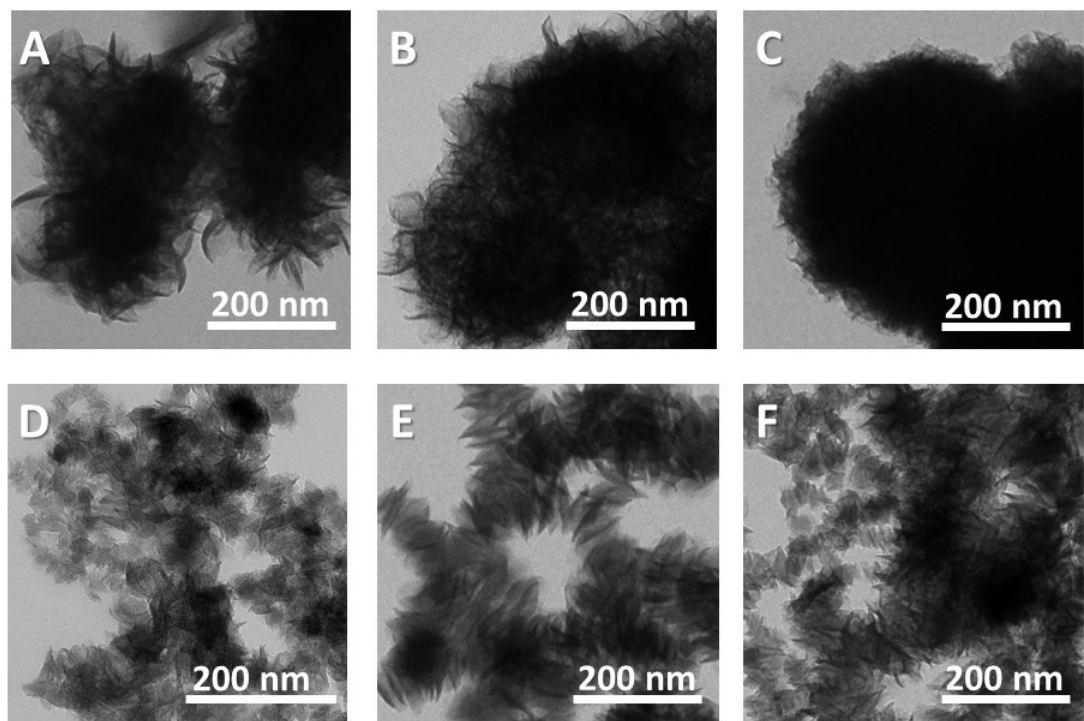


Fig. S4 TEM of (A) La_2S_3 -MoS₂-1, (B) La_2S_3 -MoS₂-2, (C) La_2S_3 -MoS₂-3, (D) La_2S_3 -MoS₂-4, (E) La_2S_3 -MoS₂-5, (F) La_2S_3 -MoS₂-6.

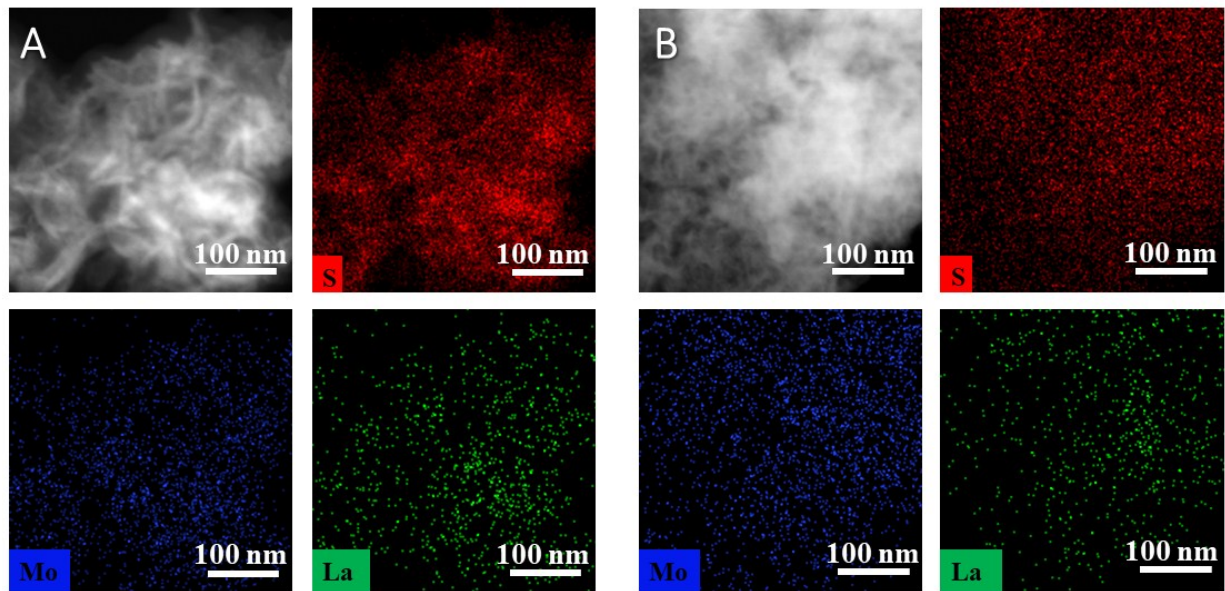


Fig. S5 TEM-EDX element mapping of La, S and Mo for (A) La₂S₃-MoS₂-1 and (B) La₂S₃-MoS₂-3.

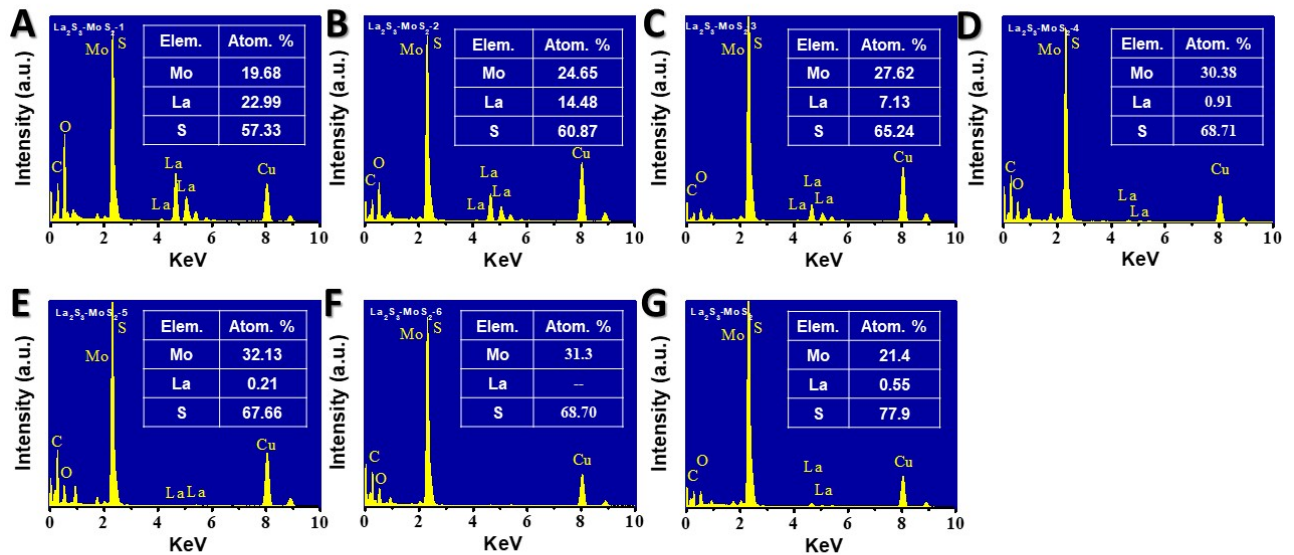


Fig. S6 TEM-EDX spectra of (A) La₂S₃-MoS₂-1, (B) La₂S₃-MoS₂-2, (C) La₂S₃-MoS₂-3, (D) La₂S₃-MoS₂-4, (E) La₂S₃-MoS₂-5, (F) La₂S₃-MoS₂-6, (G) La₂S₃-MoS₂.

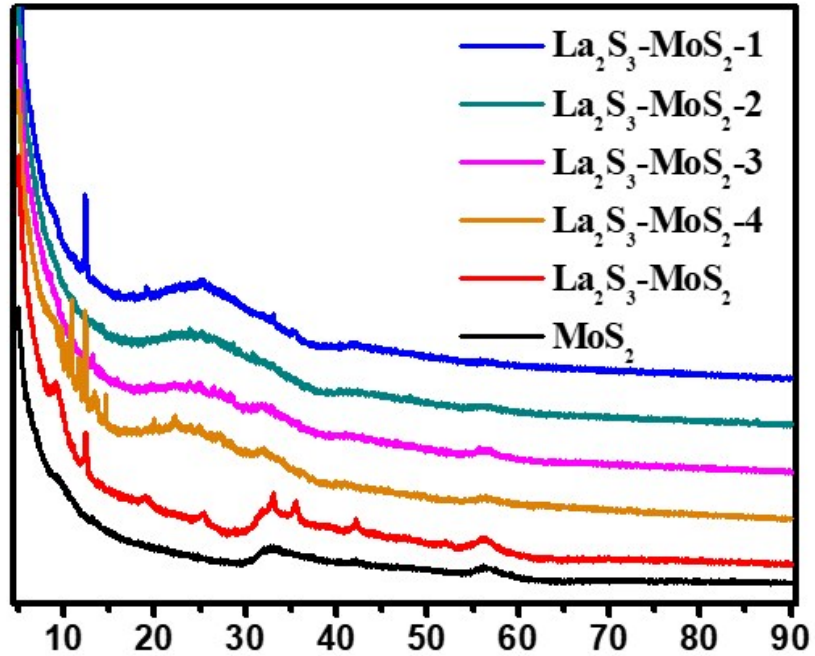


Fig. S7 XRD of $\text{La}_2\text{S}_3\text{-MoS}_2$ -1, $\text{La}_2\text{S}_3\text{-MoS}_2$ -2, $\text{La}_2\text{S}_3\text{-MoS}_2$ -3, $\text{La}_2\text{S}_3\text{-MoS}_2$ -4, $\text{La}_2\text{S}_3\text{-MoS}_2$ and MoS_2

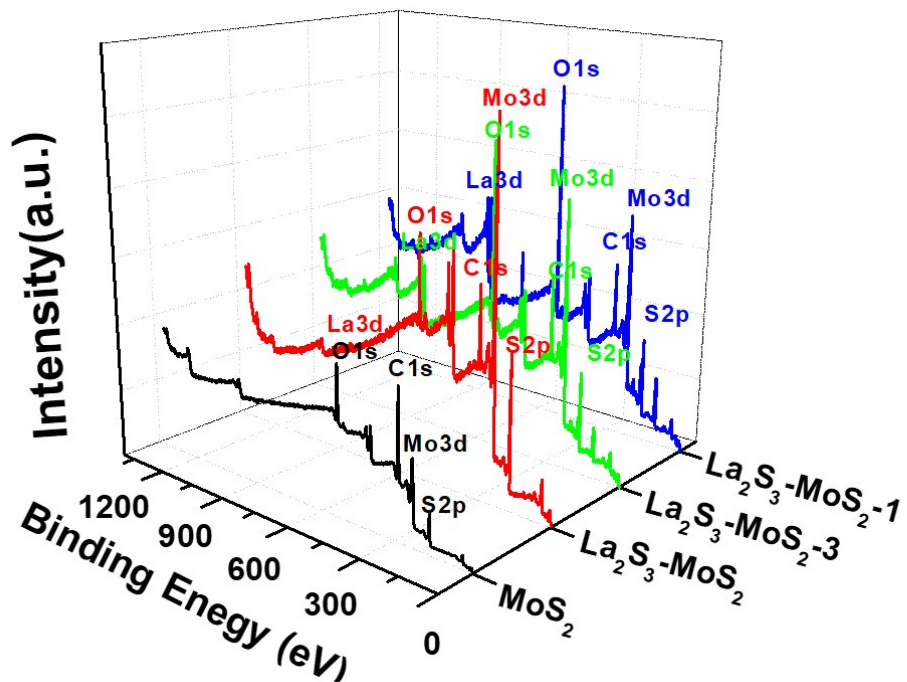


Fig. S8 Survey XPS spectra of $\text{La}_2\text{S}_3\text{-MoS}_2$ with different La content.

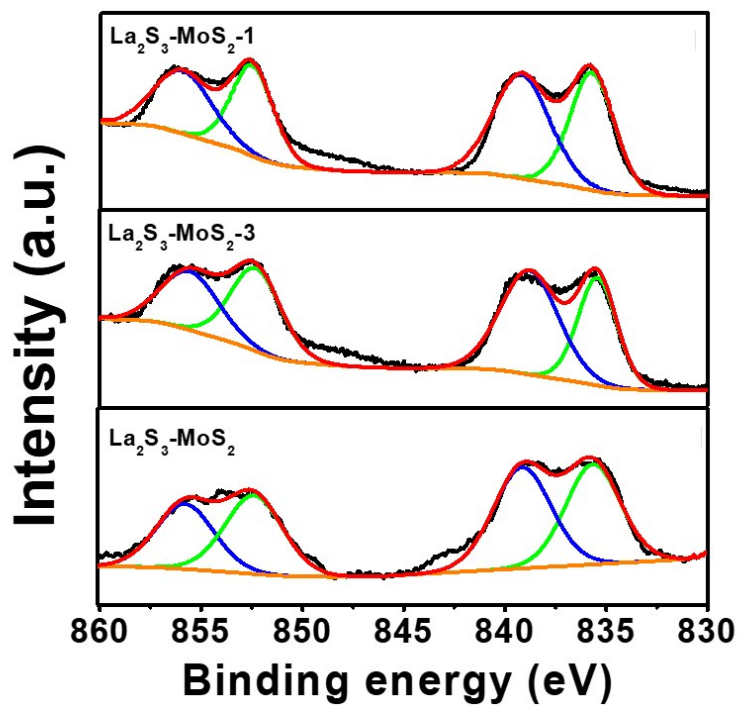


Fig. S9 High-resolution XPS spectra of La

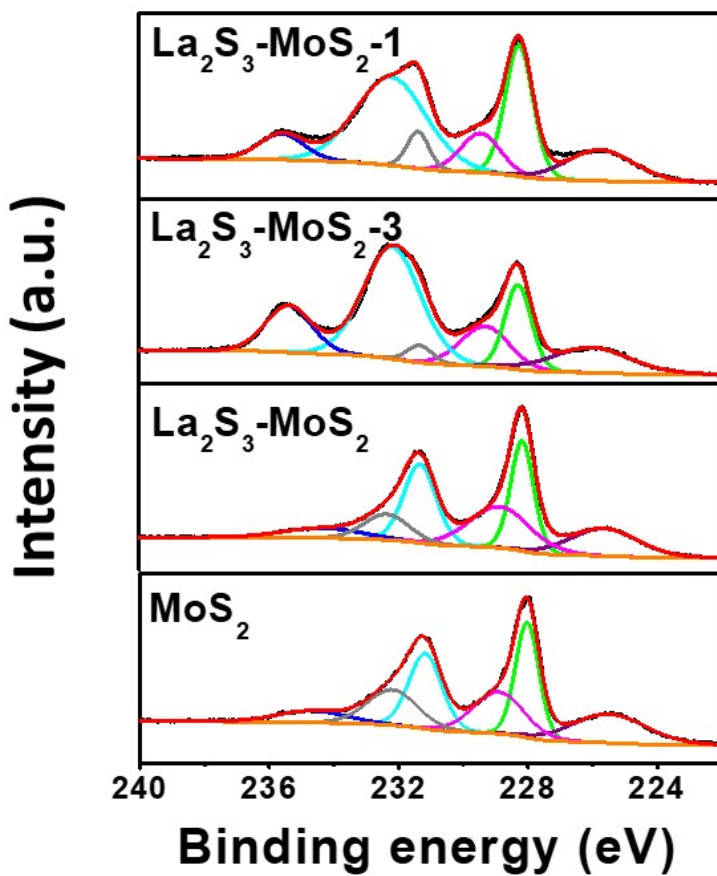


Fig. S10 High-resolution XPS spectra of Mo

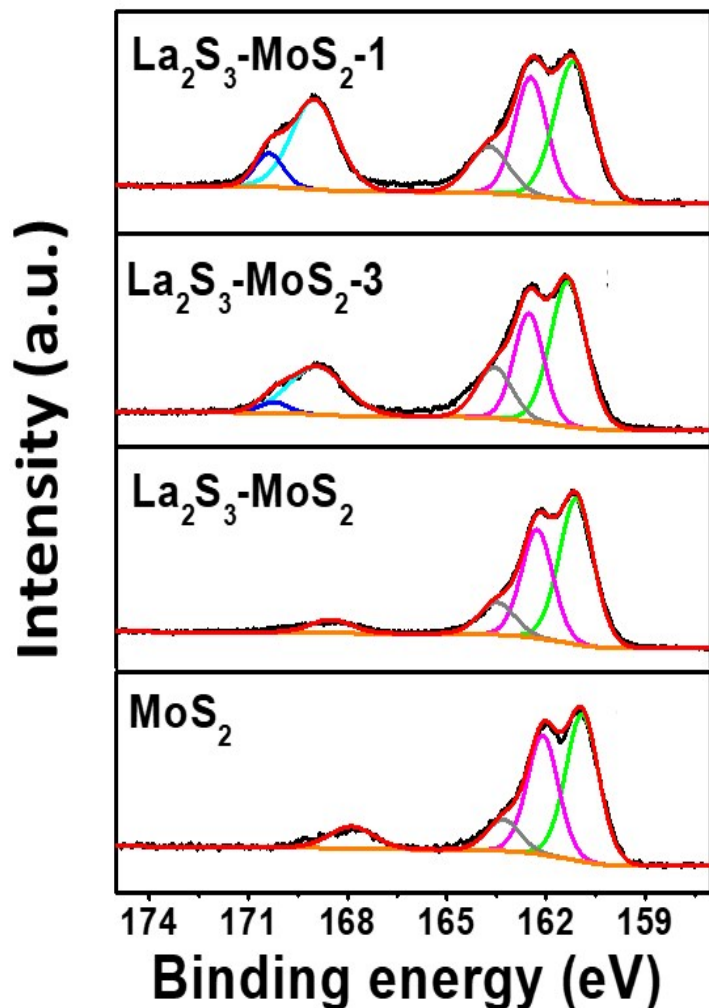


Fig. S11 High-resolution XPS spectra of S

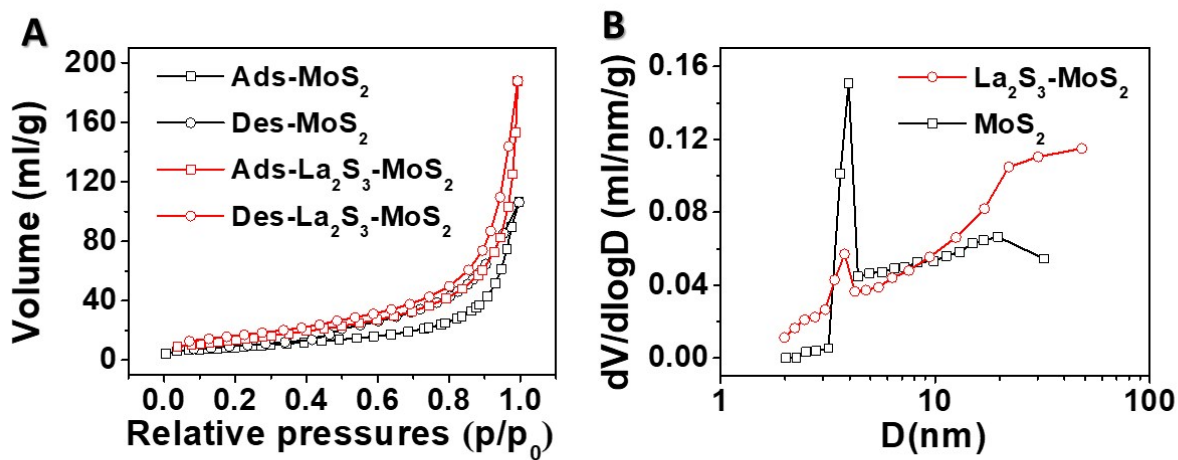


Fig. S12 (A) Nitrogen adsorption-desorption isotherms of La₂S₃-MoS₂ and MoS₂ (B) the corresponding pore distribution

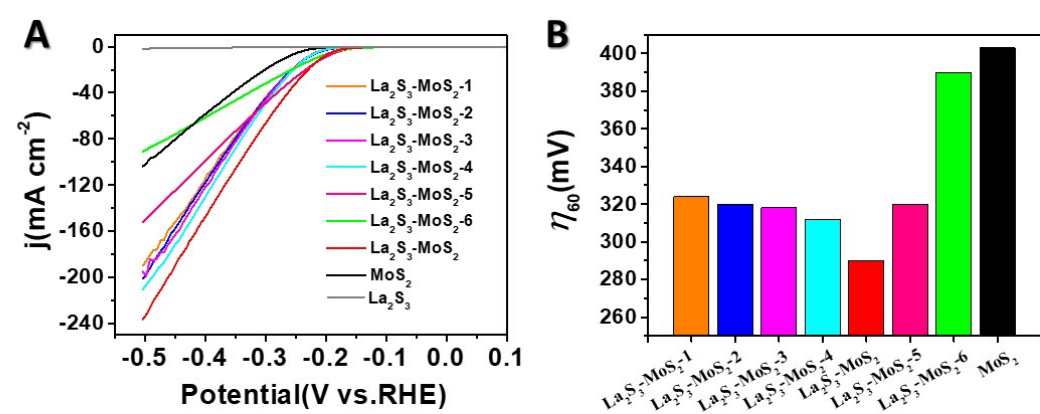


Fig. S13 (A) Polarization curves of samples for HER with different La content. (B) Overpotentials for the HER current density of 60 mA cm^{-2} .

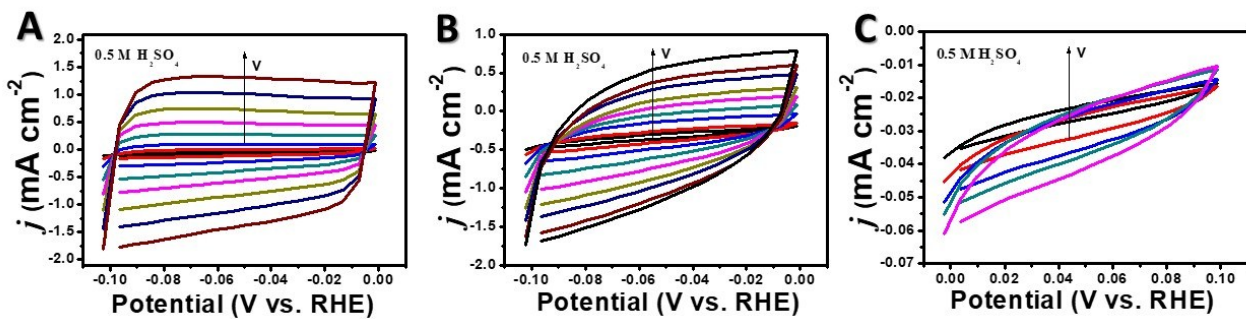


Fig. S14 Electrochemical active surface area analysis by the cyclic voltammetry scans in a non-Faradaic potential range at different scan rate (A) $\text{La}_2\text{S}_3\text{-MoS}_2/\text{C}$, (B) MoS_2/C and (C) Com-MoS₂/C.

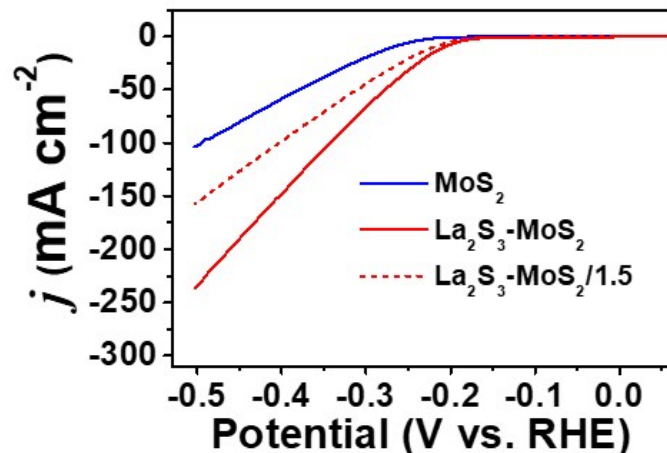


Fig. S15 Comparison of specific activities of $\text{La}_2\text{S}_3\text{-MoS}_2$ and MoS_2 for HER. Based on BET test and

double-layer capacitance (C_{dl}) test, the electrochemical surface area (EASA) of La_2S_3 -MoS₂ is 1.5 times that of pristine MoS₂. We then normalized the current densities of La_2S_3 -MoS₂ by dividing by 1.5.

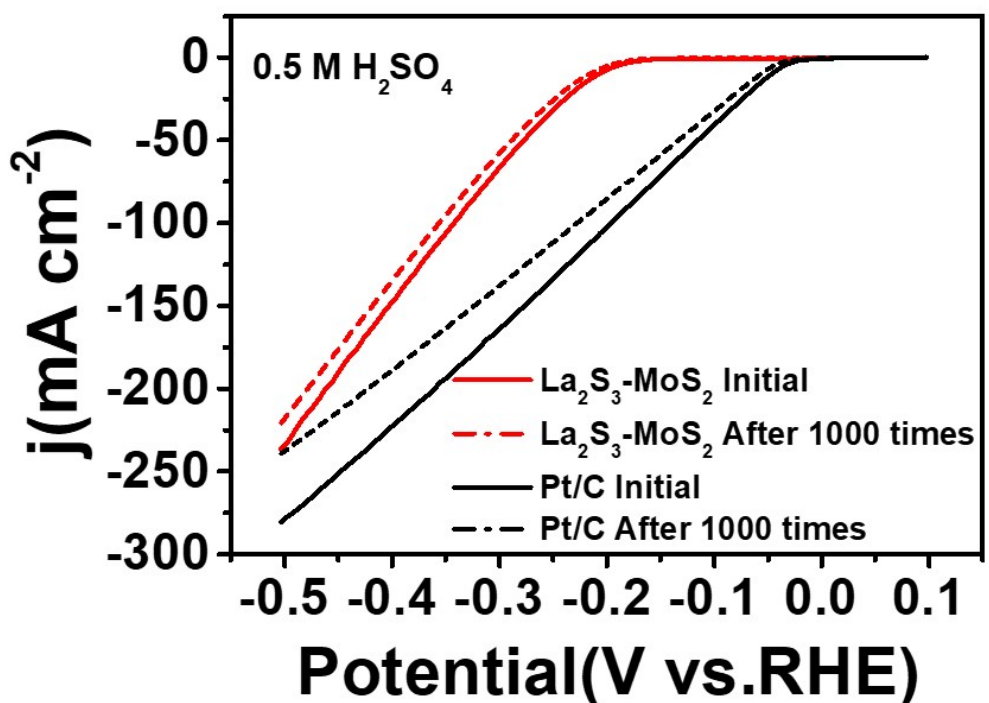


Fig. S16 LSV curves of La_2S_3 -MoS₂ and Pt/C obtained before and after 1000 times LSV scans,

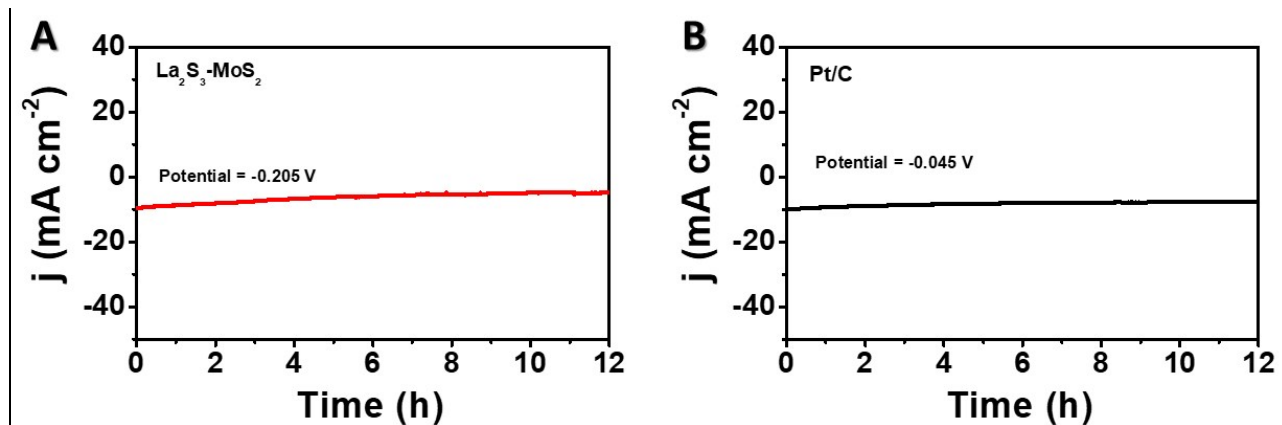


Fig. S17 Chronoamperometric responses (i-t) collected on the (A) La_2S_3 -MoS₂ and (B) Pt/C at the applied overpotentials of 205 mV and 45 mV, respectively.